Title:

Solute diffusion in gels: thirty years of simulations

Authors and affiliation

Manuel Quesada-Pérez[1], Alberto Martín-Molina[2,3*]

1. Departamento de Física, Escuela Politécnica Superior de Linares, Universidad de Jaén, 23700, Linares, Jaén, Spain
2. Departamento de Física Aplicada, Universidad de Granada, Campus de Fuentenueva sn, 18071 Granada, Spain
3. Instituto Carlos I de Física Teórica y Computacional, Universidad de Granada, Campus de Fuentenueva sn, 18071 Granada, Spain

***** Corresponding author.

Tel: 0034 958 242736

Fax: 0034 958 243214

E-mail address: almartin@ugr.es (A. Martín-Molina)

Abstract (500 words)

In this review, we present a summary of computer simulation studies on solute diffusion in gels carried out in the last three decades. Special attention is paid to coarse-grained simulations in which the role of steric and electrostatic interactions on the particle diffusion can be evaluated. In addition, other important characteristics of particle diffusion in gels, such as the stiffness of the gel structure and hydrodynamic interactions, can be taken into account through coarse-grained simulations. Emphasis is placed on how simulation results help to test phenomenological models and to improve the interpretation experimental results. Finally, coarse-grained simulations have also been employed to study the diffusion controlled release of drugs from gels. We believe that scientific advances in this line will be useful to better understand the mechanisms that control the diffusive transport of molecules in a wide variety of biological systems.

Keywords (3): Diffusion, gel, coarse-grained simulations

Contents:

1. Introduction and background

The diffusion of solute molecules in gels plays a fundamental role in different technological, industrial and biological processes. For instance, the precise knowledge of the diffusion coefficient is required in drug delivery for an accurate prediction of diffusion-controlled release kinetics and the proper control of drug dosage. The comprehensive understanding of solute diffusion in gels is also essential in separation processes (e.g., gel permeation chromatography [1] or membrane separation [2]). Biopolymer-based hydrogels (such as mucus) constitute selective barriers that regulate the passage of some macromolecules through them [3]. Oher examples of applications of solute diffusion in gels are those related to diffusion in hydrogel contact lenses [4] and encapsulation of cells in hydrogels for biomedical applications [5,6].

At the late nineties, a plethora of theoretical models for solute diffusion in gels were reviewed by Amsden,[7] and Masaro and Zhu.[8] These theories can be classified into three main categories: i) free volume theories; ii) obstruction theories; ii) hydrodynamic theories. Free volume theories assume that the solute particles move by jumping into voids formed in the solvent space by the redistribution of the free volume. This mechanism mainly governs the diffusion of molecules whose size is less than the characteristic dimensions of these voids. Obstruction theories focused on the hindrance caused by the impenetrable polymer chains, paying special attention to the geometry of the network. Finally, hydrodynamic theories consider that polymer chains enhance the frictional drag on the solute by slowing down the fluid around them. Obstruction and hydrodynamic models are often based on idealized pictures of the polymer backbone. According to Amsden, obstruction theories are particularly suitable for gels made of rigid fibers (such as alginate- or agarose-based hydrogels)[7]. On the other hand, the diffusion in gels composed of flexible chains can be described with the help of hydrodynamic theories. Recent experiments with heterogeneous gels seem to support this hypothesis.[9] Unfortunately, their underlying models often include unknown solvent-solute interaction parameters limiting their capacity of prediction. In any case, here we restrict ourselves to those models derived from computer simulations or tested by means of these techniques.

It is not surprising that many theorists have developed models based on excluded volume interactions (also known as steric interactions) since these forces are always present. Steric interactions are also the basis of size filtering: solute particles can travel long distances through a hydrogel if they are small enough to seep through the voids between polymer chains. This sounds quite intuitive and appealing. However, Lieleg et al. claimed that the notion of size filtering is not enough to fully understand the permeability properties of mucus hydrogels [10]. In fact, these researchers found that acidic mucin hydrogels are much more selective than the neutral ones. Thus, they concluded that electrostatic forces between diffusing particles and mucin polymers control the permeability of mucin hydrogels to a great extent. This is what they call interaction filtering. Moreover, when mucin chains are negatively charged, they can interact via hydrophobic and electrostatic forces as well as via the formation of disulfide bonds [11]. Accordingly, no wonder so many scientists are looking for the physical mechanism explaining how particles facilitate their own diffusion in a polymer gel giving rise to a perfect filter. For

instance, recently it has been found that binding-mediated mechanisms can contribute to enhance diffusion of particles in a gel [12].

Under this scenario, coarse-grained (CG) simulations, on their own or in a combination with theoretical approaches, become a powerful tool to test the previously cited theories and to improve their capability of prediction. In this sense, CG simulations have been widely used in the last three decades to simulate polymer networks as well as gels and microgels (see [13,14] and references cited therein). Moreover, CG simulations could be used to predict the impact of formulation and processing parameters on the kinetics of drug release. For instance, Rapp et al. used CG Brownian Dynamics simulations together with fluorescence recovery after photobleaching (FRAP) experiments, to study strand exchange and polymer self-diffusivity in associative protein hydrogels [15]. More recently, Schneible et al. have used all-atom molecular dynamics simulations to obtain the CG interaction potentials between drug molecules and chitosan chains by following the force matching method [16,17]. Thanks to the combination of simulation and experiments, the authors go deeper into the design of chemotherapeutic hydrogels to combat cancer.

Accordingly, the aim of this review article is to provide an update of the findings on solute diffusion in gels obtained through CG simulations. In particular, the work comprises i) simulations of uncharged gels in order to analyse the role of steric obstruction; ii) simulations of charged gels in which electrostatic interactions control the diffusion of charged solutes to a great extent; iii) explicit simulations of drug release from nanometer-sized gels.

2. Models and techniques

CG models of gels in solute diffusion.

Many questions regarding gels involve length and time scales that considerably exceed those that can be treated in atomistic simulations. For that reason, different levels of coarse-graining have been employed to achieve simplified representations of reality. Most of the CG models used in solute diffusion considered that the polymer network was rigid (its constituents did not fluctuate). In three pioneering works, Johansson et al. constructed wormlike chains consisting of spherical beads (Fig. 1 a) [18–20]. Netz and Dorfmüller generated a diamond-like lattice connecting randomly distributed nodes through biased self-avoiding walks with certain degree of randomness [21]. In a subsequent work, Netz and Dorfmüller modeled gel-like systems as i) sets of randomly placed points; ii) points distributed along the sides of isolated and merged cubes [22]. Miyata also constructed a cubic lattice made of immobile small spheres [23,24] beads (Fig. 1 b). Again, a rigid cubic lattice was employed by Hansing, Netz and their coworkers. In this case, the lattice was comprised of straight and infinite rods [25–27]. Hansing and Netz also employed arrays of infinite rods in the three spatial directions to study the influence of spatial disorder on diffusion in gels. Such disorder was introduced by randomly displacing the fibers from their position in a perfect cubic lattice [28] beads (Fig. 1 c). A similar cubic structure made of rectangular rods was also employed by Miyamoto et al. to model an agar-gel [29]. These researchers obtained diffusion coefficients of sugars in agar-gel that agree with those available in the literature. Other authors have modeled gels are networks of rigid straight fibers with

different degrees of alignment [30,31]. As the reader can imagine, macroscopic gels cannot be simulated to their full extent. The simulation cell usually contains just an inner portion of the gel, which is periodically replicated. Periodic boundary conditions are applied in this case.

In the works mentioned so far, the gel-like structure was rigid. Thus, the effect of polymer chain flexibility on solute diffusion could not be addressed. Just a few surveys have considered flexible structures. Some authors have employed a network of spheres initially placed at the nodes of a cubic lattice connected to their nearest neighbors by Hookean springs beads (Fig. 1 d) [32–34]. It should be stressed, however, that this model does not consider the existence of polymer chains.

A more realistic model of crosslinked flexible polymer chains was employed by Kamerlin and Elvingson [35]. The network was constructed by connecting randomly placed tetravalent crosslinkers through polymer chains made of beads. It should be mentioned, however, that these authors employed spherical boundary conditions instead of the conventional periodic boundary conditions. In this representation, the cubic 3D simulation cell is transformed into the surface of a 4D sphere. Consequently, distances must be measured along the great circle geodesics.

Lattice models (in which space is discretized) were also employed to simulate diffusion in the interphase cell nucleus, which is filled with chromatin fibers [36,37]. In their first work, Wedemeier et al. modeled this fibrous medium as three different static structures: i) randomly distributed obstacles; ii) a random walk; iii) a self-avoiding random walk [36]. In a second work, they considered the flexibility of the chromatin fibers through a combination of the bond fluctuation method and the Metropolis algorithm [37].

As can be concluded, a wide variety of CG models has been employed in simulations of solute diffusion in gels. However, just a few of these models[23,24,27,35] are inspired in some way by the bead-spring model of chemically crosslinked gels. According to this representation of reality, each polymeric chain is modeled as a sequence of spherical beads characterized by their radius and charge. The ends of these chains are connected to crosslinker molecules. Excluded volume forces between beads are usually included through the hard sphere potential or the Weeks-Chandler-Andersen (WCA) potential:

$$u_{WCA}(r) = \begin{cases} 4\varepsilon_{WCA}\left(\frac{(R_i+R_j)^{12}}{r^{12}} + \frac{(R_i+R_j)^{6}}{r^{6}} + \frac{1}{4}\right) & r \le 2^{1/6}(R_i + R_j) \\ 0 & r > 2^{1/6}(R_i + R_j) \end{cases} \quad (1)$$

Here ε_{WCA} is the energy characterizing the strength of this repulsive interaction potential and R_i stands for the radius of species *i.*

The flexibility of the polymeric chain is simulated connecting monomers and crosslinkers through elastic bonds. The elastic forces associated to them can be included in the model through harmonic interaction potentials [38–41]:

$$u_{bond}(r) = \frac{k_{bond}}{2}(r - r_0)^2 \quad (2)$$

where r is the center-to-center distance between the beads, k_{bond} is the elastic constant and r_0 is the equilibrium bond length. Other authors prefer nonlinear potentials, such as the so-called finite extension nonlinear elastic potential.[42] A value of $k_{bond} = 0.4$ N/m was employed in some CG simulations of polyelectrolyte gels [38,39,43–45]. Other values for the elastic constant have also be proposed but in all cases, k_{bond} has to be chosen in such a way that thermal fluctuations undergone by monomers must be smaller than their diameter [42,46,47]. The inclusion of elastic bonds between monomers allows simulating flexible gels but requires much longer computational times. Maybe for that reason, rigid gels have been mostly preferred in simulations of solute diffusion.

According to the CG models of polyelectrolyte gels developed in the 2000s, small ions are explicitly treated and charged species interact via pure Coulomb forces. However, in simulations of solute diffusion in gels, electrostatic interactions are usually included through screened Debye-Hückel-like potentials and small ions arising from the dissociation of chemical groups on the polyelectrolyte chains and electrolytes in solution are taken into account only implicitly through the screening Debye parameter.[20,23–28] For instance, Johansson *et al.* employed the Debye-Hückel (DH) potential:[20]

$$u_{DH}(r) = \frac{q_i q_j}{4\pi\varepsilon_r\varepsilon_0}\frac{\exp(\kappa R_i)}{1+\kappa R_i}\frac{\exp(\kappa R_j)}{1+\kappa R_j}\frac{\exp(-\kappa r)}{r} \qquad (3)$$

Here q_i and R_i are the charge and the radius, respectively, of species i (charged monomers or solute particle in this case), $\varepsilon_r\varepsilon_0$ is the dielectric permittivity of the solvent and κ is the Debye screening parameter. We should keep in mind that: i) these authors considered a point-like solute and a rigid gel; ii) small ions are not explicitly included. For these reasons, the DH potential is applied only to monomer-solute electrostatic interactions.

One of the main advantages of CG models is the generality of conclusions, which can be valid to a great extent for a huge variety of systems regardless their chemical composition. It is worth mentioning, however, that molecular dynamics simulations at atomistic level can also be employed if we are interested in specific substances. In fact, Wu et al. studied the diffusion of chloride, sodium and rhodamine in poly(ethylene glycol) diacrylate (PEGDA) gels through molecular dynamics [48]. These authors focused on the effect of the crosslinking degree, which can be defined as the ratio of crosslinker molecules to the total number of monomers (other definitions are also possible). In the simulations performed by Wu et al., the crosslinking degree ranged from 0.004 to 0.025, whereas the mesh size ranged from 2.28 to 5.49 nm. It should be mentioned, however, that broader ranges of crosslinking degree and mesh size have been explored in simulations within CG models of crosslinked gels. For instance, Miyata studied diffusion in gels with crosslinking degrees and mesh sizes ranging from 0.002 to 0.110 and from 9.6 to 72 nm, respectively.[24]

Diffusion coefficient

Before presenting the expressions that govern the diffusion of solute in gels, we must start from solute particles that execute a Brownian motion in a 3D medium. Herein, the mean

square displacement (MSD) of the particles, $\langle \Delta r^2 \rangle$, is calculated from averaging over a statistical ensemble and is a linear function of time t:

$$\langle \Delta r^2 \rangle = 6Dt \quad (4)$$

Here, D is the coefficient in the medium. This relationship, which was first derived by Einstein, is the fundamental link between the microscopic and the macroscopic descriptions of diffusion. Additionally, it allows us to compute the diffusion coefficient by calculating the MSD of a tracer particle along a wide set of simulated trajectories. Strictly speaking, computer simulations provide a self-diffusion coefficient. In contrast to collective diffusion, which involves the simultaneous transport of many particles induced by concentration gradients, self-diffusion is related to the dynamics of single particles and can take place without the presence of concentration gradients. In addition, it should be mentioned, that in many complex fluids (such as crowded media or gels), Eq. 4 only holds for very short times. After a certain time, the MSD becomes proportional to t^{β}. This regime is known as anomalous diffusion. The reader interested in anomalous diffusion is referred to the review by Metzler et al. [49]. In many cases, $0 < \beta < 1$, which means that this motion is slower than Brownian motion. For that reason, this situation is also known as subdiffusion. However, anomalous diffusion is often a transient regime and at long times the MSD is again described by Eq. 4 but with a different diffusion coefficient. In these cases, short- and long-time diffusion coefficients can be defined.

In any case, the computation of MSD requires averaging over a large number of trajectories, which can be generated using different simulation techniques. Many of the simulations are performed through Brownian Dynamics (BD), an implicit solvent simulation method based on the generalized Smoluchowski equation. In the absence of hydrodynamic interactions, the displacement of particle j during a time step Δt is given by [50]:

$$\Delta r_j = \sqrt{2D_0 \Delta t} N(0,1) + D_0 F_j \Delta t / k_B T \quad (5)$$

where D_0 is the free diffusion coefficient of the particle in the solvent (which can be estimated from the Einstein-Stokes relationship), $N(0,1)$, is a random number generated according to a Gaussian distribution of zero mean and unit standard deviation, F_j is the force exerted on particle j, k_B is Boltzmann's constant and T the absolute temperature. The first term on the right side of this expression is due to the Brownian diffusion process experienced by a particle immersed in a fluid as a result of collisions with the molecules of that fluid. On the other hand, the second term includes the effect of forces. Apart from Eq. 5, there is no equation for the particle velocity because the time step is assumed to be so long that nearly all velocity information is lost from one-time step to the next.

Although BD seems to be particularly suitable for simulation of diffusive processes, some authors have also employed the Monte Carlo (MC) method [21,22,36,37]. One should keep in mind, however, that time is not explicitly considered in conventional MC schemes. Consequently, the MSD is monitored as a function of the number of executed MC steps.

To end this section, it should be mentioned that just a few researchers have considered hydrodynamic interactions in their simulations of solute diffusion in gels. In these cases, Stokesian Dynamics (SD) was preferred. In BD, hydrodynamic interactions can be approximated

as a Stokesian friction or coarsely treated through a diffusion tensor. In contrast, SD is an implicit solvent simulation method that rigorously considers interparticle hydrodynamic interactions [51]. One of the main disadvantages is its low adaptability to complex particle shapes or geometries.

3. Uncharged gels: the role of steric obstruction

At the early nineties, Johansson et al. performed BD simulations of a solute particle in a gel made of rigid worm-like chains [18,19]. Hydrodynamic interactions were not considered. In fact, they only considered excluded volume interactions between the solute and the hard spheres forming the polymer chains. Johansson and Löfroth employed the algorithm developed by Cichoki and Hinsen [52] for systems of hard spheres to compute the ratio of the long-time diffusion coefficient in a gel to the free diffusion coefficient in the solvent, D/D_0. The influence of the radius of the solute particle (R_s), the polymer volume fraction (φ), the polymer radius (R_p), and the persistence length of the chains were systematically studied [19]. In our opinion, it is worth stressing the effect of the polymer radius. Johansson and Löfroth corroborated that the diffusion coefficient decreases when the radius of the polymer fiber decreases (provided that the polymer volume fraction remains fixed). In other words: thin polymer fibers contribute more to steric hindrance than thick fibers (as long as the polymer volume fraction is the same). This feature was justified considering that as the polymer radius increases the distances between the chains also increase and thus, a faster diffusion is reached [19].

Johansson and Löfroth also proved that their simulation results can be predicted to a great extent by a hard sphere theory that provide the following expression:

$$D/D_0 = \exp(-\alpha) + \exp(\alpha) \cdot \alpha^2 E_1(2\alpha) \qquad (6)$$

Here $\alpha = \varphi(1 + R_s/R_p)^2$ and E_1 is the exponential integral. The agreement between the simulation data and the predictions of this expression was quite satisfactory for α<1. On the other hand, the theory overestimates D/D_0 (which we will refer to as relative diffusivity) for high polymer volume fractions and/or large solute particles. However, simulation data could be better reproduced by the following phenomenological expression [19]:

$$D/D_0 = \exp(-0.84\alpha^{1.09}) \qquad (7)$$

It is quite instructive to compare the predictions of Eq. 7 and recent experimental data for adenosine triphosphate (ATP) molecules [53], whose radius is 0.633 nm, and dextran molecules with radii of 1.00 and 1.90 nm in PEGDA gels [54]. In the experiments with ATP, the polymer volume fraction varied from 0.06 to 0.30. Three polymer volume fractions were studied in the two cases of dextran molecules (0.03, 0.05 and 0.08). The relative diffusivity measured for these samples is plotted as a function of α in Fig. 2. The computation of this parameter requires the radius of the polymer chain, R_p, which was estimated from the molecular weight (M_m) and the density (ρ_m) of the corresponding monomer (ethylene glycol) as $R_p \approx \sqrt[3]{0.74 \cdot 3M_m/4\pi N_A \rho_m}$, where N_A is Avogadro's number, turning out to be 0.27 nm.

As can be inferred from Fig. 2, Eq. 7 provides acceptable predictions of relative diffusivity for $\alpha < 1$. The discrepancies between theory and experiment grow with α. In particular, Eq. 7 significantly underestimates the diffusion coefficient of the solute with the largest radius (1.90 nm). We should keep in mind that Eq. 7 was derived from simulation data of rigid worm-like chains whereas certain degree of flexibility is expected for real PEGDA chains. Consequently, Fig. 2 suggests that the flexibility of the chains is a determining factor for high polymer volume fractions and particularly for large solute sizes, but its influence is scarce for low α–values.

Netz and Dorfmüller also investigated excluded volume effects on solute diffusion in uncharged and rigid gels. Two different structures were considered: i) a distribution of randomly placed points (as model of disordered media); ii) points placed along the sides of isolated and merged cubes (as a better approximation to gel-like structure) [22]. Although these structures were made of points, excluded volume effects were present due to the finite size of the solute particle. In the case of randomly placed points they concluded that D/D_0 is also given by the expression derived and tested by Johansson and Löfroth [19]. It should be stressed, however, that the meaning of the dimensionless parameter α is now different. For disordered media, $\alpha = 4\pi n_p R_s^3/3$, where n_p is the number density of points. For the cubic gel-like structures, these authors did not propose an analytical expression but they concluded that knowing the distribution of the obstacles in the space allows making a very satisfactory prediction of the diffusion behavior for different solute sizes.

These authors also paid special attention to anomalous diffusion and stated that this phenomenon is pronounced if the radius of the solute particle is larger than 80% of the mean pore radius. This finding agreed with the results that they had previously observed for rigid diamond-like structures: when the solute diameter becomes comparable to the pore size the exponent characterizing the growth of the MSD diverges [21]. Netz and Dorfmüller also found that the time evolution of the MSD can be split into three regimes (as long as the solute particle does not become trapped): normal diffusion at short times, anomalous diffusion (as transition) and normal diffusion again at long times. Recently, Ghosh *et al.* have studied the anomalous diffusion of a tracer particle attracted by the obstacles forming a crowded medium [55]. These researchers concluded that the diffusive regime strongly depends on the strength of the attractive interaction between the tracer particle and the obstacles and their volume fraction. More specifically, increase, the transient subdiffusion regime progressively extends over a larger time window when these parameters increase.

As mentioned before, Wedemeier et al. also considered different static structures in their study on diffusion in crowed media of chromatin fibers [36]. They concluded that different conformations lead to different diffusive behaviors. In particular, the more homogeneous the distribution of obstacles, the lower the diffusion coefficient. These authors also observed that chromatin fibers of different chain length exhibit almost the same diffusion coefficient if the volume fraction remains constant.

Stylianopoulos et al. focused on the effect of the fiber orientation [30]. Four fibrous structures made of rigid rods with different degrees of alignment ranging from nearly anisotropic to perfectly aligned rods were considered. These authors concluded that the overall diffusion coefficient is not significantly affected by the degree of alignment. However, spatial

anisotropy generates anisotropic diffusion process. This is logical and had been observed in simulations of charged gels by Johansson et al.(see next section) [20].

As pointed out above, Hansing, Netz and their coworkers modeled the gel as a cubic lattice made of rigid straight rods [25–27]. Although this model was mainly developed for charged gels, it was also applied to neutral networks. In this case, the predictions of the model clearly deviates from experimental relative diffusivities measured by Tong et al.[56]. The model predicts that the relative diffusivity of purely steric systems describes an almost linear function in the range of polymer volume fractions studied, whereas experimental data describe a convex function that resembles an exponential decay [27]. Later, Hansing and Netz improved their original model in two independent ways. On the one hand, they introduced different degrees of disorder displacing the fibers from their ordered positions in the cubic lattice [28]. Good agreement between Eq. 7 and their simulation results was reported when the degree of disorder was moderate. In other words, the diffusive behavior of their disordered model of gel was similar to that of a model with randomly oriented fibers. On the other hand, Hansing and Netz introduced the effect of hydrodynamic interactions [27]. In the case of neutral gels, their simulation data agree with the heuristic correction for Eq. 7 proposed by Philips [57]:

$$D/D_0 = \exp(-\pi\varphi^m)\exp(-0.84\alpha^{1.09}) \qquad (8)$$

where $m = 0.174\ln(59.6R_p/R_s)$. The first exponential is the correction attributed to hydrodynamic interactions. In addition, the inclusion of hydrodynamic forces considerably improved the agreement between simulations and experiments. Since significant discrepancies were reported in the absence of hydrodynamic interactions, these researchers concluded that *their* original model was substantially affected by these forces. In fact, the diffusion coefficient was approximately halved for polymer fractions around 0.04. But this does not necessarily mean that the impact of hydrodynamic interactions will be so important in any other model and/or circumstances. Fig. 2 provides an illustrative example of this. Eq. 7 does not include hydrodynamic interactions and, in spite of this, gives us a good prediction of the relative diffusivity of ATP in PEGDA-based gels for low α-values. This clearly suggests that the impact of hydrodynamics must not be significant in this case. We therefore think that the cubic lattice employed by these researchers could be responsible for the overestimation of the diffusion coefficient when hydrodynamic forces are absent but this lattice would also amplify the reduction that this interaction causes in diffusion. Both effects would cancel each other.

The effect of hydrodynamic forces can depend not only on the geometry of the model but also on the procedure employed to implement them. Blanco et al. simulated the long-time diffusion of proteins in crowded media through BD [58]. On the one hand, hydrodynamic interactions were implemented through the Rotne-Prager-Yamakaya diffusion tensor [59]. In this case, these authors observed that these forces only bring about a slight decrease in the relative diffusivity. On the other hand, Blanco et al. computed the long-time diffusion coefficient replacing the free diffusion coefficient appearing in Eq. 5 by the short-time diffusion derived by Tokuyama [60–62], which includes the effect of hydrodynamic interactions. A considerable reduction in the relative diffusivity was reported. According to Blanco et al., this difference can be attributed to short-range hydrodynamic forces (neglected by the Rotne-Prager-Yamakaya diffusion tensor).

The effect of the flexibility of the gel-like structure on solute diffusion in uncharged gels was also investigated through CG simulations by some authors. For instance, Teixeira and Licinio considered diffusion in the system formed by beads interacting through harmonic potentials with their neighbors [32]. An analogous model was used by Zhou and Chen who found that: i) the diffusion coefficient decreases with increasing the elastic constant characterizing the harmonic potential (as expected); ii) solute particles trapped in a rigid lattice could diffuse if the elastic constant is low enough [33].

A similar system of coupled oscillators was also employed by Sandrin et al. [34]. They tried to justify the diffusion coefficients measured for dextran molecules of different molecular weights and sizes diffusing through a polyacrylamide hydrogel. The agreement between experiments and simulations was achieved only after including an attractive contribution to the solute-obstacle interaction. We should bear in mind that this model does not explicitly consider the existence of crosslinked polymeric chains. Perhaps a more realistic model would not require such attractive forces.

Wedemeier et al. did explicitly consider polymeric chains in their lattice simulations of a medium filled with chromatin fibers. But these chains were not chemically crosslinked. In fact, they were able to diffuse [37]. These authors concluded that chain dynamics does not significantly modify the diffusion process of small solute particles. However, chain diffusion does facilitate the transport of large particles. These conclusions can help us to understand why Eq. 7 (derived for rigid chains) gives acceptable predictions for low polymer volume fractions and small solutes but dramatically fails for large particles.

Probably, the most realistic model of crosslinked flexible polymeric chains is the model used by Kamerlin and Elvingson, briefly commented above. They performed simulations in static (rigid) and dynamic (flexible) networks and also found that dynamic networks facilitates the diffusion of large particles [35]. In addition, Kamerlin and Elvingson determined the pore size of the network introducing a large number of expanding bubbles at random positions and registering the size that prevents them from diffusion. From these values, they concluded that diffusion in flexible networks is possible even for solute sizes well above the mean pore diameter.

In relation to the atomistic simulations performed by Wu et al. for sodium ion, chloride ion and rhodamine in PEGDA gels with several degrees of crosslinking [48], it should be mentioned here that the predictions of the obstruction model proposed by Amsden [63] agree with their simulation results only if different corrections to the Einstein-Stokes relationship are employed to estimate ionic radii. The correction proposed for chloride and sodium ions approximately doubles the sizes initially obtained from this relationship. However, the correction employed for rhodamine reduces its ionic radius. Unfortunately, the use of different corrections from case to case considerably reduces the capability of prediction of the model.

4. Charged gels: the role of electrostatic interactions

Johansson and Löfroth also pioneered the simulation of diffusion of ions in rigid charged gels [20]. Ordered and disordered networks were generated. The ordered networks consisted

of parallel straight chains arranged on a square lattice whereas randomly oriented worm-like chains formed the disorder ones. In both cases, polyelectrolyte chains were made of charged spherical units (beads). The electrostatic interaction between monovalent ions and these beads were modeled through a Debye-Huckel potential. The radius and charge density of two differently charged conformations of ι-carrageenan (a natural polysaccharide) were employed in simulations for comparison with experiments. Concerning the solute, the study of Johansson and Löfroth was restricted to monovalent ions (more specifically, the choline ion). In the case of ordered networks, these authors computed the coefficient for the diffusion parallel to the chains and for the diffusion in the radial direction. They found that: i) both coefficients could be successfully predicted by the Smoluchowski-Poisson-Boltzmann theory [64]; ii) the diffusion in the radial direction is more affected by the electrostatic attraction between the solute particle and the fibers. The results obtained for disordered networks from simulations and experiments showed qualitative agreement. The quantitative discrepancies were justified arguing that experiments and simulations were not performed at the same concentrations of added salt (1 mM and 10 mM, respectively). Johansson and Löfroth also compared the diffusion coefficients measured for choline and glycerol (ion and neutral molecule of similar size) in different carrageenan-based gels to find out the relevance of electrostatic effects in diffusion. Their experimental results reveal that electrostatic attraction slows down diffusion. It is somewhat surprising that they did not compare the diffusion coefficients obtained from simulations for charged and uncharged solutes of the same size obtained to tackle this task.

Miyata et al. simulated the diffusion of a charged particle in a polyelectrolyte network made of immobile small spheres along the sides of a cubic lattice [23,24]. They focused on slightly charged networks since the fraction of charged beads varied from 0 to 0.20. The electrostatic interaction between charged beads and the solute (screened by their corresponding electric double layers) was taken into account through the potential derived by Wiese and Healy. According to their results, the self-diffusion coefficient of the solute particle can significantly decrease as a result of the attractive electrostatic force between the particle and the network. In fact, the diffusion coefficient can be two (and even more) orders of magnitude smaller than the free diffusion coefficient. In practice, such a large reduction means that electrostatic forces can bring about the immobilization of charged particles. In any case, it should be mentioned that the charge of the solute particle studied in these simulations was +8*e* (*e* denotes the elementary charge). Miyata et al. did not vary this parameter. However, it plays an important role because Johansson and Löfroth did not observed any electrostatic entrapment for monovalent ions [20].

Miyata et al. also found that the solute particle should overcome a free energy barrier when they moved along the polyelectrolyte network. In addition, these authors showed that their results collapse onto a universal curve if they are represented as a function of this energy barrier (E_b). In fact, this master curve is given by the following function [24]:

$$D/D_0 = (E_b/k_BT)^2 \exp(-E_b/k_BT) \,/\big(1-\exp(-E_b/k_BT)\big)^2 \qquad (9)$$

The effect of electrostatic repulsive forces when charged particles diffuse through an array of rigid parallel fibers with charge of the same sign was studied by Stylianopoulos et al.

[31]. Their model took steric, electrostatic and hydrodynamics interactions into account. According to their results, the repulsive electrostatic interactions can substantially slow down the diffusive movement of the solute particle if the fiber size is comparable to the Debye screening length. These authors also concluded that the diffusion of charged particles is more affected in the direction parallel to the fibers, which is in agreement with the behavior reported by Johansson and Löfroth for attractive forces [20].

Hansing, Netz and their coworkers carried out a systematic study including both repulsive and attractive electrostatic forces between the solute particle and a cubic lattice made of rigid rods [25,26]. The main parameters charactering the corresponding potential energy are the Debye screening length (l_D) and its strength (U_0), which can be estimated by:

$$U_0/k_BT = 2Z_p\lambda l_B I_0(p/2l_D)K_0(p/2l_D)\exp(p/2l_D) \quad (10)$$

Here Z_p is particle charge number, λ is the linear charge density of the rods (expressed as number of elementary charges per unit of length), l_B is the Bjerrum length, I_0 and K_0 are the modified Bessel functions and $p = 2(R_s + R_p)$. U_0 is positive for repulsive forces and negative for attractive forces. Another important parameter of the model is the lattice constant (b), which can be thought of as the distance between crosslinkers in a gel.

Fig. 3 summarizes most of the main results of this work. In this figure, D/D_0 is plotted as function of p/b for different U_0-values (attractive and repulsive forces) and $l_D = 0.1b$. The case of purely steric forces ($U_0 = 0$) was also included for comparison. As can be seen, the five curves plotted in Figure 3 merge into one for $/b > 0.6$, which means that steric forces are dominant under this condition. On the other hand, electrostatic effects play a key role if $p/b < 0.4$. In this case, both attractive and repulsive forces slow down diffusion, in agreement with the results reported for arrays of rigid fibers reported by Johansson and [20] Löfroth and Stylianopoulos et al. [31]. In fact, it can be concluded from Fig. 3 that neutral particles overall diffuse faster than charged particles of the same size. However, Fig. 3 clearly reveals that the slowdowns caused by attractive and repulsive interactions present quite different features. For strongly repulsive forces ($U_0 = 10k_BT$ and $20k_BT$) and $p/b < 0.4$, the quotient D/D_0 decreases just slightly. This means that the relative diffusivity is insensitive to the particle size. As Hansing et al. claim, this behavior was reported in experiments. Xu et al. studied the diffusivity of PEG coated polystyrene particles in fresh bovine vitreous [65]. The relative diffusivity of particles with diameters ranging from 100 to 500 nm turned out to be of the order of 0.5, which can be reproduced by simulations with $U_0 = 10k_BT$.

On the other hand, it can be inferred from Fig. 3 that the relative diffusivity increases with the particle size for strongly attractive forces ($U_0 = -10k_BT$ and $-20k_BT$) and $p/b < 0.4$. Again, this had been observed in experiments. Lai et al. studied the diffusivity of PEG coated polystyrene particles with diameters 100, 200 and 500 nm in cervicovaginal mucus [66]. They reported that the relative diffusivity of 100-nm particles was considerably smaller than the others. This behavior was qualitatively reproduced from simulations with $U_0 = -10k_BT$.

Finally, it should be stressed that, according to Fig. 3, the relative diffusivity falls to zero for $U_0 < -10k_BT$ if the solute particle size is small enough. In other words, strongly attractive interaction can immobilize the solute, in agreement with the findings by Miyata et al. for a rigid

cubic lattice. Hansing et al. attributed this immobilization to the fact that solute particles remain near the intersections of the rods. At this point, we might wonder i) if U_0-values larger than $10k_BT$ in magnitude can be representative of small molecules and ions, like many drugs; ii) if these conclusions remain valid for flexible networks.

The rigid cubic lattices employed by Hansing, Miyata and their respective coworkers are highly ordered structures. As mentioned before, Hansing and Netz explored what happened if certain degree of disorder was introduced in such a lattice [28]. In the case of attractive electrostatic forces between the solute and the rods, they found a new trapping mechanism. In disordered networks, particles are trapped in regions of high local fiber density due to the deep well of potential energy that the accumulation of fibers generates. If electrostatic forces are repulsive, solute particle are confined in regions with low local fiber density and the slowest diffusion is achieved for intermediate degrees of disorder. Hansing and Netz also observed that highly disordered networks are provided with random passageways of low fiber concentration that improve solute diffusivity (as compared to moderately disordered structures). Hansing and Netz also compared the predictions of their model to experimental relative diffusivities of Alexa488 (a negatively charged fluorophore) in positive and negatively charged and neutral dextran-based gels. A highly degree of disorder improved the agreement between experiment and simulations. These authors also concluded that chain flexibility might reduce the differences between ordered and disordered networks. Similarly, Hansing et al. investigated the diffusion of charged particles in gels with a random distribution of attractive and repulsive electrostatic interaction sites inside the gel [67]. In particular CG simulations were used to analyze the translational diffusion coefficients of Alexa488 in hydrogels consisting of positive DEAE-dextran and negative CM-dextran polymer chains, measured by fluorescence correlation spectroscopy (FCS). Their findings revealed that particles were strongly localized near attractive sections of the fiber network and therefore attractive interactions mostly determine the diffusive behavior of the particles in systems with mixed attractive and repulsive interactions. In this sense, they concluded that gels with mixed interactions trap particles nearly as effectively as gels with purely attractive interactions. In addition, they found that the effect of interaction disorder and spatial disorder on the diffusive behavior of the solute is qualitatively similar in both cases [68].

Hansing and Netz also assessed the impact of hydrodynamic interactions in the predictions of their model for charged gels [27]. According to their results, the effect of these interactions is greater in the presence of attractive electrostatic forces whereas repulsive interactions decrease the hydrodynamic effect compared to purely steric gels. This is logical since the solute particles remain far from the fibers when they repel each other. These authors also observed that hydrodynamic interactions also improved the agreement between simulations and experimental diffusivities reported for Alexa488 in dextran-based gels. In our opinion, however, the particular geometry employed by these researchers in their model might overestimate the influence of hydrodynamic forces.

To complete this section, it is important to remark the possible deformations of the gel structure upon particle diffusion. For instance, Shin et al. used molecular dynamics computer simulations to analyze the degree of hydrogel compaction caused by binding of polymeric chains to a pathogen particle incorporated in the hydrogel [69]. Particularly, the authors demonstrated

that the presence of electrostatic binding between positively charged viruses and DNA chains bundles incorporated in a responsive hydrogel induces a mechanical response of the polyelectrolyte network.

Finally, a summary of the main characteristics of the systems discussed in the sections 3 and 4 is shown in Table 1.

5. Simulating drug release

The comprehension of the mechanisms involved in drug release and their mathematical modelling are essential to speed up the development of advanced delivery platforms [70]. In this sense, CG simulations could be used to predict the impact of formulation and processing parameters on the kinetics of drug release. After having computed the diffusion coefficient of a given solute inside a gel, it is possible to predict the release kinetics from solutions of Fick's law. Alternatively, we could explicitly simulate drug release provided that the border of the gel and part the outer medium are included in the simulation cell. This can be easily done in the case of polymeric networks with nanometric dimensions (at least in one of the spatial directions) since the diffusing particle can reach the border of the polymeric matrix. In fact, a few researchers have monitored the fraction of drug released as a function of time (or MC steps) simulating solute diffusion. The first simulations of the release kinetics were performed in a lattice model, in which space is discretized in a number of sites [71–73]. The sites belonging to the polymeric matrix were initially occupied by drug molecules or excipient, and drug molecules could jump into adjacent sites as long as they were empty. The inner structure of the gel was not considered. It should also be mentioned that the release process was simulated under perfect sink conditions. This means that drug particles were removed as soon as they left the polymeric matrix. The fraction of drug release was computed as a function the simulation steps since the MC method was employed. Kosmidis et al. studied the release from cylindrical matrices and concluded that the kinetics can be fitted by the so-called Weibull function. Its parameters were related to the specific surface of the cylinder [71]. In a subsequent work, Kosmidis et al. compared the Weibull function and Mittag-Leffler function [72]. Both expressions can describe the release kinetics up to 85% of the release process. However, both models underestimate the fraction of drug released at larger times. Villalobos et al. employed the same technique to study the release from spherical matrices. In this case, the Weibull function can fit up to 90% of the release [73]. These authors were also able to determine the amount of drug trapped in the matrix, which was function of the initial drug load.

Maroto-Centeno and Quesada-Pérez also simulated the release from a rigid and neutral gel of nanometric size (nanogel) [74], but their technique was quite different from that used in the above mentioned studies [71–73]. First, the model of nanogel explicitly considered the polymeric chains, the crosslinkers joining them and the excluded volume interactions between any pair of constituents of the system (monomers, crosslinkers and solute particles). On the other hand, the technique proposed by Cichoki and Hinsen [52] was employed instead of MC to simulate the solute diffusion. In this way, the drug release can be monitored as a function of real time. Fig. 4 shows the fraction of drug released from a nanogel whose mean radius (R_n) is 17.34

nm as a function of the dimensionless time $D_0 t/R_n^2$ (where t denotes time) for two diameters of drug particles (1 and 2 nm) [74]. As can be seen, the first 60% of the release curve is almost linear in log-log plot, but the slope depends on the drug size. This means that this part of the release kinetics can be described by a power law whose exponent depends on the solute size due to excluded volume interactions whereas the classical theory of drug release predicts that this exponent is constant for diffusion-controlled release from a given polymeric matrix. Moreover, Maroto-Centeno and Quesada-Pérez found that this kinetic exponent also depends on the initial drug concentration inside the nanogel. In addition, it is worth stressing that the predictions obtained from the assumption of perfect sink conditions for gels of a few tens of nanometers can considerably differ from those obtained assuming that drug molecules can freely diffuse after leaving the nanogel. In fact, these researchers also proved that the concentration of drug in the immediate neighborhood of the nanogel changes with time and becomes negligible only at the end of the release process.

As mentioned before, these simulations were restricted to rigid and neutral nanogels. In practice, however, nanogels are usually flexible and charged structures. Therefore, they electrostatically interact with many charged solutes. It would be quite interesting to extend this preliminary work to the case of flexible and charged nanogels. Perhaps this might shed light on some puzzling findings. For instance, some researchers have experimentally determined the release kinetics of anticancer drugs (such as doxorubicin and 5-fluorouracil) previously loaded in pH-responsive nanogels, whose charge and size depends on pH.[75–77] Cazares-Cortés et al. have concluded that the release kinetics speeds up if the nanogel shrinks.[77] In contrast, Álvarez-Bautista et al. have claimed that the drug is released more rapidly when the nanogel swells.[76] And, surprisingly, Aguirre et al. have found that the effect of the nanogel size on the kinetics is negligible.[75] Controlled release necessarily involves a comprehensive understanding of this disparity of results. Apart from electrostatic interactions, the presence of hydrophobic forces between the polymer chains of collapsed gels or nanogels and some drugs should not be ignored in future simulations or models of diffusion.

Finally, BD simulations have been used to study uptake and release of polyelectrolytes within core–shell responsive microgels by Gelissen et al. [78]. In particular these authors simulated microgels with a cationic core and an anionic shell, which were loaded with anionic polystyrene sulfonate of different molecular weights to investigate the effect of their chain length on the uptake and release process. According to their results, polyelectrolyte can be released through of the anionic shell, being the size of the guest molecules of major importance for the release mechanism (the release of long-chain polyelectrolytes was much more efficient compared to the release of short-chain polyelectrolytes) [78].

5. Conclusions

Here we summarize the most relevant conclusions obtained from CG simulations applied to solute diffusion of in gels:

- Phenomenological theories based on power law expressions of the diffusion coefficient of particles on neutral gels, provides acceptable predictions for small solutes (in relation to the polymer size).
- The flexibility of the chains is a determining factor for large solute sizes (in the case of uncharged gels).
- The effect of hydrodynamic forces on the diffusion molecules in neutral gels can depend not only on the geometry of the model but also on the procedure employed to implement them.
- Charged particles diffuse slower than uncharged particles regardless the sign of the gel charge. However, oppositely charged gels are more effective in slowing down charged particles than similarly charged gels.
- The effect of hydrodynamic forces on the particles in charged gels is greater in the presence of attractive electrostatic interactions.
- CG simulations show that the release curve of small solutes in a rigid gel can be qualitatively described by a power law whose exponent depends on the solute size and its concentrations.
- In the case of polyelectrolyte in core-shell polyampholyte gels, BD simulations point out that negative chains can be released through likely charged shell. This feature becomes more significant for the case of long-chain polyelectrolyte.

Acknowledgements

This study has been partially financed by the "Consejería de Conocimiento, Investigación y Universidad", Junta de Andalucía and European Regional Development Fund (ERDF), ref. SOMM17/6105/UGR.

Table 1:

Summary of the main characteristics of the systems discussed in the sections 3 and 4.

Ref	Solute radius range (nm)	Rigid/flexible chains	Charged-uncharged Gel	Hydrodynamic interactions	Binding	Polymer volume fraction	Crosslinked network
18	0,5 - 1,6	Rigid	Uncharged	No	No	0,001 - 0,026	No
19	0,5-3,0	Rigid	Uncharged	No	No	0,005 -0,050	No
20	0 (point-like ions)	Rigid	Charged	No	No	0,001 - 0,026	No
21	0,05 - 3,0	Rigid	Uncharged	No	No	~ 0,06 - 0,20	Yes
22	0,2 - 1,0	Rigid	Uncharged	No	No	~ 0,017 - 0,130	No
23	1,95	Rigid	Charged	No	Electrostatic	~ $7 \cdot 10^{-4}$ - 0,011	Yes
24	1,95	Rigid	Charged	No	Electrostatic	~ $5 \cdot 10^{-5}$ - 0,003	Yes
25	1,9	Rigid	Both	No	Electrostatic	~ 0,082	Yes
26	1,9	Rigid	Both	No	Electrostatic	~ 0 - 0,044 and 0,082	Yes
27	~ 0,4 - 1,8	Rigid	Both	Yes	Electrostatic	< 0,12	Yes
28	~ 0,4 - 1,8	Rigid	Both	No	Electrostatic	< 0,12	Yes
31	5,6 and 5,8	Rigid	Charged	Yes	No	0,005 - 0,08	No
33	2.5	Flexible	Both	No	No	0,0005 - 0,272	Yes
34	0,56 - 40	Flexible	Uncharged	No	No	0,005 and 0,06	Yes
35	1,00 - 15,00	Flexible	Uncharged	No	No	0,02 - 0,05	Yes
48	0,33 - 0,49	Flexible	Uncharged	No	No	0,09 - 0,25	Yes
55	Point-like tracer	Rigid	Uncharged	No	Yes	$5{,}2 \cdot 10^{-4}$ - 0,52	No
58	2,33 - 4,90	Rigid	Uncharged	Yes	No	0 - 0,4	No
67	0,74	Rigid	Charged	No	Electrostatic	~ 0,025 -0,05	Yes

Figure Captions

Figure 1: Some of the models of gel employed in simulations of solute diffusion: a) worm-like chains. Reprinted with permission from reference [18]. Copyright (1991) American Chemical Society; b) chains of small beads along the sides of a cubic lattice. Reprinted with permission from [24]. Copyright (2012) The Physical Society of Japan; c) rods along the sides of a cubic lattice. Reprinted with permission from reference [25]. Copyright (2015) Elsevier; d) beads connected by Hookean springs.

Figure 2: Relative diffusivity (D/D_0) as a function of $\alpha = \varphi(1 + R_s/R_p)^2$ for ATP (black squares), dextran molecules with radius of 1.00 nm (red circles) and dextran molecules with radius of 1.90 nm (blue triangle). The prediction of Eq. 7 is also plotted (line).

Figure 3: Relative diffusivity (D/D_0) as a function of p/b for different U_0-values and $l_D = 0.1b$. Data extracted from reference [26].

Figure 4. Fraction of drug released from a nanogel whose mean radius (R_n) is 17.34 nm as a function of the dimensionless time $D_0 t/R_n^2$ for two diameters of drug particles (1 and 2 nm) [74]. The dashed line marks the first 60% of the release.

Figures

a)

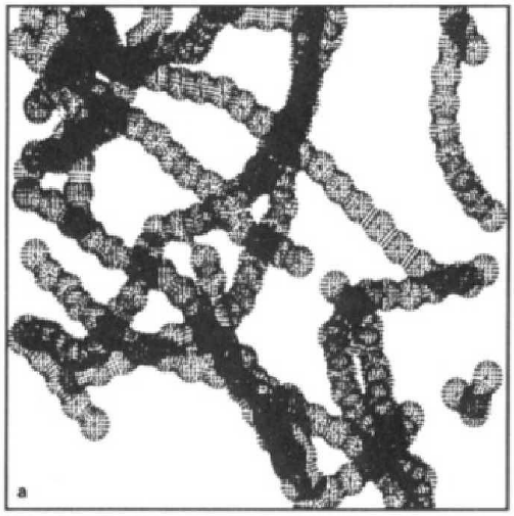

b)

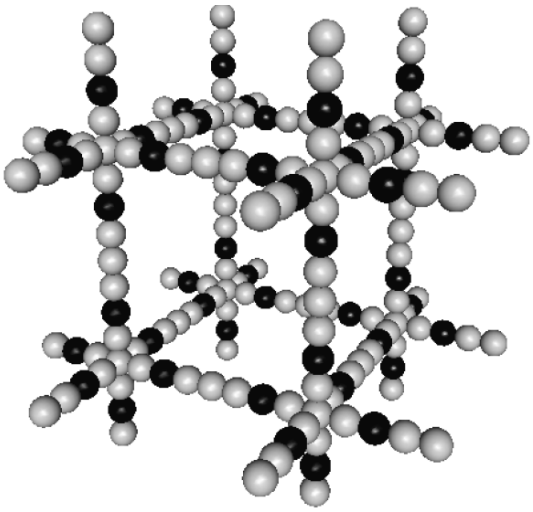

c)

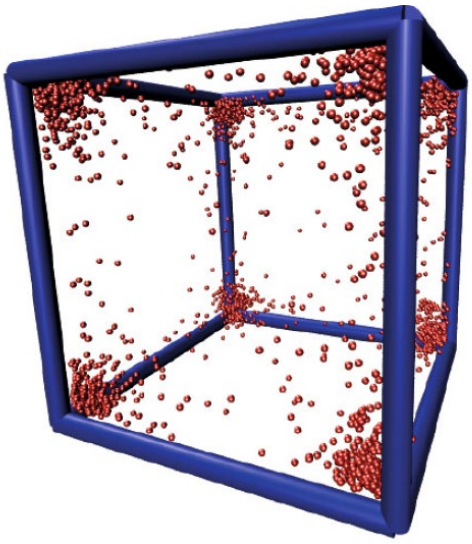

d)

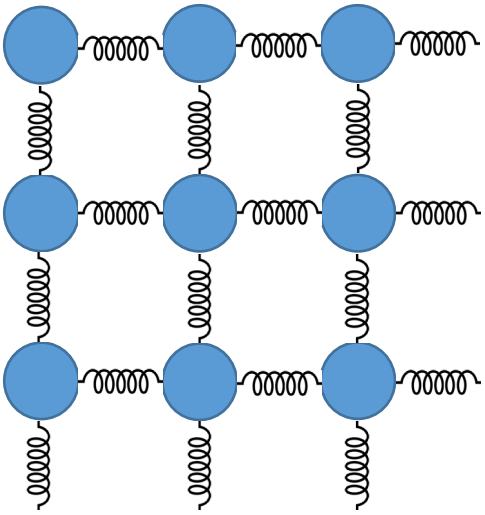

Figure 1

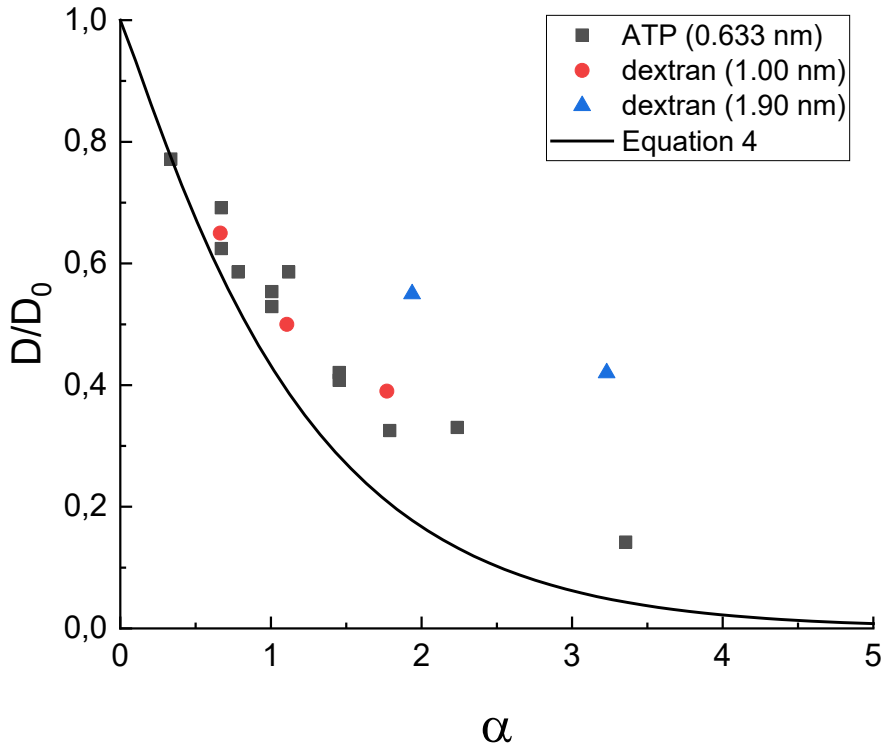
ATP (0.633 nm)
dextran (1.00 nm)
dextran (1.90 nm)
Equation 4
D/D0
α
1,0
0,8
0,6
0,4
0,2
0,0
0
1
2
3
4
5

Figure 2

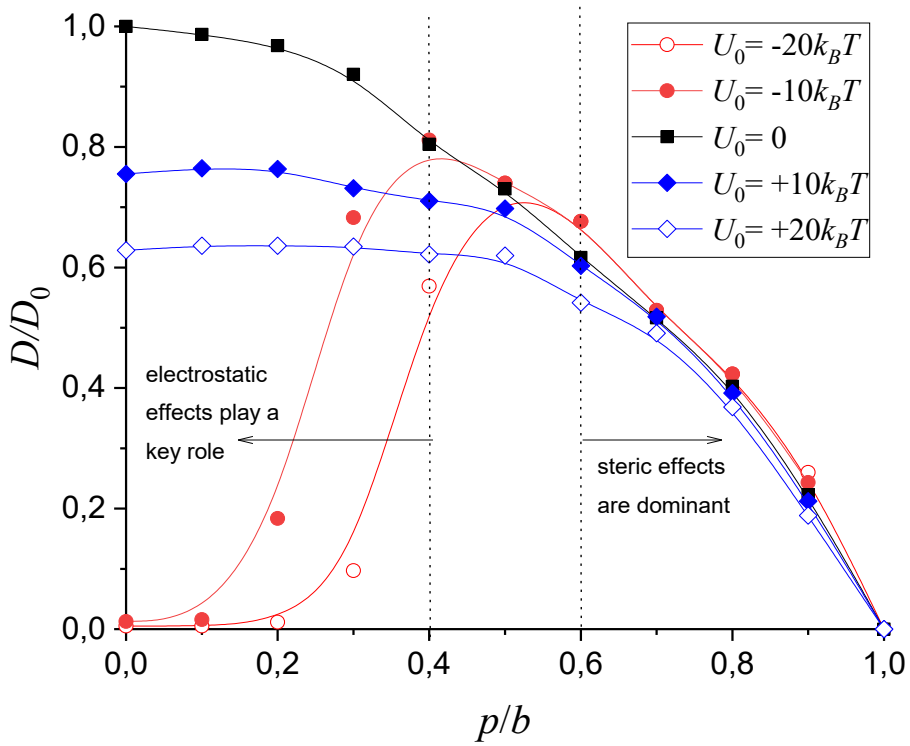
1,0
0,8
0,6
0,4
0,2
0,0
0,0
0,2
0,4
0,6
0,8
1,0
D/D0
p/b
U0= -20kBT
U0= -10kBT
U0= 0
U0= +10kBT
U0= +20kBT
electrostatic
effects play a
key role
steric effects
are dominant

Figure 3

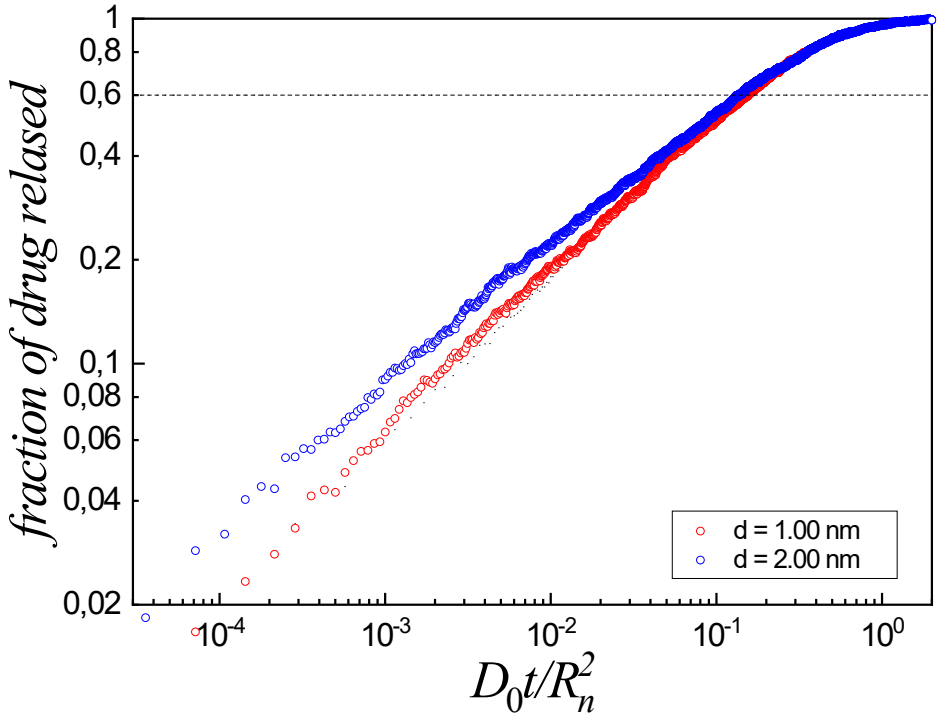
fraction of drug relased
1
0,8
0,6
0,4
0,2
0,1
0,08
0,06
0,04
0,02
10-4
10-3
10-2
10-1
100
D0t/Rn2
d = 1.00 nm
d = 2.00 nm

Figure 4

References.

[1] Hermans JJ. Role of diffusion in gel permeation chromatography. J Polym Sci Part A-2 Polym Phys 1968;6:1217–26. https://doi.org/10.1002/pol.1968.160060702.

[2] Peppas NA, Bures P, Leobandung W, Ichikawa H. Hydrogels in pharmaceutical formulations. Eur J Pharm Biopharm 2000;50:27–46. https://doi.org/https://doi.org/10.1016/S0939-6411(00)00090-4.

[3] Casalini T, Perale G. From Microscale to Macroscale: Nine Orders of Magnitude for a Comprehensive Modeling of Hydrogels for Controlled Drug Delivery. Gels 2019;5:28. https://doi.org/10.3390/gels5020028.

[4] Liu DE, Kotsmar C, Nguyen F, Sells T, Taylor NO, Prausnitz JM, et al. Macromolecule sorption and diffusion in HEMA/MAA hydrogels. Ind Eng Chem Res 2013;52:18109–20. https://doi.org/10.1021/ie402148u.

[5] Lu S, Anseth KS. Release Behavior of High Molecular Weight Solutes from Poly(ethylene glycol)-Based Degradable Networks. Macromolecules 2000;33:2509–15. https://doi.org/10.1021/ma9915024.

[6] Drury JL, Mooney DJ. Hydrogels for tissue engineering: scaffold design variables and applications. Biomaterials 2003;24:4337–51. https://doi.org/https://doi.org/10.1016/S0142-9612(03)00340-5.

[7] Amsden B. Solute diffusion within hydrogels. Mechanisms and models. Macromolecules 1998;31:8382–95. https://doi.org/10.1021/ma980765f.

[8] Masaro L, Zhu XX. Physical models of diffusion for polymer solutions, gels and solids. Prog Polym Sci 1999;24:731–75. https://doi.org/10.1016/S0079-6700(99)00016-7.

[9] Tokuyama H, Nakahata Y, Ban T. Diffusion coefficient of solute in heterogeneous and macroporous hydrogels and its correlation with the effective crosslinking density. J Memb Sci 2020;595:117533. https://doi.org/10.1016/j.memsci.2019.117533.

[10] Lieleg O, Vladescu I, Ribbeck K. Characterization of particle translocation through mucin

hydrogels. Biophys J 2010;98:1782–9. https://doi.org/10.1016/j.bpj.2010.01.012.

[11] Cherstvy AG, Thapa S, Wagner CE, Metzler R. Non-Gaussian, non-ergodic, and non-Fickian diffusion of tracers in mucin hydrogels. Soft Matter 2019;15:2526–51. https://doi.org/10.1039/c8sm02096e.

[12] Goodrich CP, Brenner MP, Ribbeck K. Enhanced diffusion by binding to the crosslinks of a polymer gel. Nat Commun 2018;9:4348. https://doi.org/10.1038/s41467-018-06851-5.

[13] Košovan P, Richter T, Holm C. Molecular Simulations of Hydrogels. In: Sadowski G, Richtering W, editors. Intell. Hydrogels, vol. 140, Springer International Publishing; 2013, p. 205–21. https://doi.org/10.1007/978-3-319-01683-2_16.

[14] Martín-Molina A, Quesada-Pérez M. A review of coarse-grained simulations of nanogel and microgel particles. J Mol Liq 2019;280:374–81. https://doi.org/https://doi.org/10.1016/j.molliq.2019.02.030.

[15] Rapp PB, Omar AK, Shen JJ, Buck ME, Wang Z-G, Tirrell DA. Analysis and Control of Chain Mobility in Protein Hydrogels. J Am Chem Soc 2017;139:3796–804. https://doi.org/10.1021/jacs.6b13146.

[16] Sauter J, Grafmüller A. Predicting the Chemical Potential and Osmotic Pressure of Polysaccharide Solutions by Molecular Simulations. J Chem Theory Comput 2016;12:4375–84. https://doi.org/10.1021/acs.jctc.6b00295.

[17] Schneible JD, Singhal A, Lilova RL, Hall CK, Grafmüller A, Menegatti S. Tailoring the Chemical Modification of Chitosan Hydrogels to Fine-Tune the Release of a Synergistic Combination of Chemotherapeutics. Biomacromolecules 2019;20:3126–41. https://doi.org/10.1021/acs.biomac.9b00707.

[18] Johansson L, Elvingson C, Löfroth JE. Diffusion and Interaction in Gels and Solutions. 3. Theoretical Results on the Obstruction Effect. Macromolecules 1991;24:6024–9. https://doi.org/10.1021/ma00022a019.

[19] Johansson L, LLöfroth J. Diffusion and interaction in gels and solutions. 4. Hard sphere Brownian dynamics simulations. J Chem Phys 1993;98:7471–9. https://doi.org/10.1063/1.464686.

[20] Johansson L, Skantze U, Löfroth JE. Diffusion and interaction in gels and solutions. 6. Charged systems. J Phys Chem 1993;97:9817–24. https://doi.org/10.1021/j100140a045.

[21] Netz PA, Dorfmüller T. Computer simulation studies of anomalous diffusion in gels: Structural properties and probe-size dependence. J Chem Phys 1995;103:9074–82. https://doi.org/10.1063/1.470018.

[22] Netz PA, Dorfmuller T. Computer simulation studies of diffusion in gels: Model structures. J Chem Phys 1997;107:9221–33. https://doi.org/10.1063/1.475214.

[23] Miyata T, Endo A, Ohmori T, Nakaiwa M, Kendo M, Kurumada K, et al. Brownian dynamics simulation study of self-diffusion of a charged particle in swollen counter-charged hydrogel modeled as cubic lattice. J Chem Eng JAPAN 2002;35:640–8. https://doi.org/10.1252/jcej.35.640.

[24] Miyata T. Brownian dynamics simulation of self-diffusion of ionic large solute molecule in modeled polyelectrolyte gel. J Phys Soc Japan 2012;81:1–7. https://doi.org/10.1143/JPSJS.81SA.SA010.

[25] Zhang X, Hansing J, Netz RR, Derouchey JE. Particle transport through hydrogels is charge asymmetric. Biophys J 2015;108:530–9. https://doi.org/10.1016/j.bpj.2014.12.009.

[26] Hansing J, Ciemer C, Kim WK, Zhang X, DeRouchey JE, Netz RR. Nanoparticle filtering in charged hydrogels: Effects of particle size, charge asymmetry and salt concentration. Eur Phys J E 2016;39. https://doi.org/10.1140/epje/i2016-16053-2.

[27] Hansing J, Netz RR. Hydrodynamic Effects on Particle Diffusion in Polymeric Hydrogels with Steric and Electrostatic Particle-Gel Interactions. Macromolecules 2018;51:7608–

20. https://doi.org/10.1021/acs.macromol.8b01494.

[28] Hansing J, Netz RR. Particle Trapping Mechanisms Are Different in Spatially Ordered and Disordered Interacting Gels. Biophys J 2018;114:2653–64. https://doi.org/10.1016/j.bpj.2018.04.041.

[29] Miyamoto S, Atsuyama K, Ekino K, Shin T. Estimating the Diffusion Coefficients of Sugars Using Diffusion Experiments in Agar-Gel and Computer Simulations. Chem Pharm Bull 2018;66:632–6. https://doi.org/10.1248/cpb.c18-00071.

[30] Stylianopoulos T, Diop-Frimpong B, Munn LL, Jain RK. Diffusion Anisotropy in Collagen Gels and Tumors: The Effect of Fiber Network Orientation. Biophys J 2010;99:3119–28. https://doi.org/10.1016/j.bpj.2010.08.065.

[31] Stylianopoulos T, Poh M-Z, Insin N, Bawendi MG, Fukumura D, Munn LL, et al. Diffusion of Particles in the Extracellular Matrix: The Effect of Repulsive Electrostatic Interactions. Biophys J 2010;99:1342–9. https://doi.org/10.1016/j.bpj.2010.06.016.

[32] Licinio P, Teixeira A V. Anomalous diffusion of ideal polymer networks. Phys Rev E 1997;56:631–4. https://doi.org/10.1103/PhysRevE.56.631.

[33] Zhou H, Chen SB. Brownian dynamics simulation of tracer diffusion in a cross-linked network. Phys Rev E 2009;79. https://doi.org/10.1103/PhysRevE.79.021801.

[34] Sandrin D, Wagner D, Sitta CE, Thoma R, Felekyan S, Hermes HE, et al. Diffusion of macromolecules in a polymer hydrogel: From microscopic to macroscopic scales. Phys Chem Chem Phys 2016;18:12860–76. https://doi.org/10.1039/c5cp07781h.

[35] Kamerlin N, Elvingson C. Tracer diffusion in a polymer gel: Simulations of static and dynamic 3D networks using spherical boundary conditions. J Phys Condens Matter 2016;28. https://doi.org/10.1088/0953-8984/28/47/475101.

[36] Wedemeier A, Merlitz H, Wu CX, Langowski J. Modeling diffusional transport in the interphase cell nucleus. J Chem Phys 2007;127. https://doi.org/10.1063/1.2753158.

[37] Wedemeier A, Merlitz H, Wu CX, Langowski J. How proteins squeeze through polymer

networks: A Cartesian lattice study. J Chem Phys 2009;131. https://doi.org/10.1063/1.3205100.

[38] Schneider S, Linse P. Monte Carlo simulation of defect-free cross-linked polyelectrolyte gels. J Phys Chem B 2003;107:8030–40. https://doi.org/10.1021/jp022336w.

[39] Schneider S, Linse P. Discontinuous volume transitions in cross-linked polyelectrolyte gels induced by short-range attractions and strong electrostatic coupling. Macromolecules 2004;37:3850–6. https://doi.org/10.1021/ma035512n.

[40] Edgecombe S, Linse P. Monte Carlo simulations of cross-linked polyelectrolyte gels with oppositely charged macroions. Langmuir 2006;22:3836–43. https://doi.org/10.1021/la053193i.

[41] Edgecombe S, Linse P. Monte Carlo Simulation of Polyelectrolyte Gels: Effects of Polydispersity and Topological Defects. Macromolecules 2007;40:3868–75. https://doi.org/10.1021/ma0700633.

[42] Mann BA, Holm C, Kremer K. Swelling of polyelectrolyte networks. J Chem Phys 2005;122. https://doi.org/15490310.1063/1.1882275.

[43] Ahualli S, Martín-Molina A, Quesada-Pérez M. Excluded volume effects on ionic partitioning in gels and microgels: a simulation study. Phys Chem Chem Phys 2014;16:25483–91. https://doi.org/10.1039/C4CP03314K.

[44] Edgecombe S, Schneider S, Linse P. Monte Carlo simulations of defect-free cross-linked gels in the presence of salt. Macromolecules 2004;37:10089–100. https://doi.org/10.1021/ma0486391.

[45] Quesada-Pérez M, Ahualli S, Martín-Molina A. Thermo-responsive gels in the presence of monovalent salt at physiological concentrations: A Monte Carlo simulation study. J Polym Sci Part B Polym Phys 2014;52:1403–11. https://doi.org/10.1002/polb.23576.

[46] Claudio GC, Kremer K, Holm C. Comparison of a hydrogel model to the Poisson-Boltzmann cell model. J Chem Phys 2009;131:094903. https://doi.org/094903

10.1063/1.3207275.

[47] Pérez-Mas L, Martín-Molina A, Quesada-Pérez M. Coarse-grained Monte Carlo simulations of nanogel-polyelectrolyte complexes: Electrostatic effects. Soft Matter 2020;16:3022–8. https://doi.org/10.1039/d0sm00173b.

[48] Wu Y, Joseph S, Aluru NR. Effect of cross-linking on the diffusion of water, ions, and small molecules in hydrogels. J Phys Chem B 2009;113:3512–20. https://doi.org/10.1021/jp808145x.

[49] Metzler R, Jeon JH, Cherstvy AG, Barkai E. Anomalous diffusion models and their properties: Non-stationarity, non-ergodicity, and ageing at the centenary of single particle tracking. Phys Chem Chem Phys 2014;16:24128–64. https://doi.org/10.1039/c4cp03465a.

[50] Ermak DL. A computer simulation of charged particles in solution. I. Technique and equilibrium properties. J Chem Phys 1975;62:4189–96. https://doi.org/10.1063/1.430300.

[51] Park JD, Myung JS, Ahn KH. A review on particle dynamics simulation techniques for colloidal dispersions: Methods and applications. Korean J Chem Eng 2016;33:3069–78. https://doi.org/10.1007/s11814-016-0229-9.

[52] Cichocki B, Hinsen K. Dynamic computer-simulation of concentrated hard-sphere suspensions .1. Simulation technique and mean-square displacement data. Physica A 1990;166:473–91. https://doi.org/10.1016/0378-4371(90)90068-4.

[53] Majer G, Southan A. Adenosine triphosphate diffusion through poly(ethylene glycol) diacrylate hydrogels can be tuned by cross-link density as measured by PFG-NMR. J Chem Phys 2017;146. https://doi.org/10.1063/1.4984979.

[54] Hagel V, Haraszti T, Boehm H. Diffusion and interaction in PEG-DA hydrogels. Biointerphases 2013;8:1–9. https://doi.org/10.1186/1559-4106-8-36.

[55] Ghosh SK, Cherstvy AG, Metzler R. Non-universal tracer diffusion in crowded media of

non-inert obstacles. Phys Chem Chem Phys 2015;17:1847–58. https://doi.org/10.1039/c4cp03599b.

[56] Tong J, Anderson JL. Partitioning and diffusion of proteins and linear polymers in polyacrylamide gels. Biophys J 1996;70:1505–13. https://doi.org/10.1016/S0006-3495(96)79712-6.

[57] Phillips RJ. A hydrodynamic model for hindered diffusion of proteins and micelles in hydrogels. Biophys J 2000;79:3350–3. https://doi.org/10.1016/S0006-3495(00)76566-0.

[58] Blanco PM, Via M, Garcés JL, Madurga S, Mas F. Brownian dynamics computational model of protein diffusion in crowded media with dextran macromolecules as obstacles. Entropy 2017;19. https://doi.org/10.3390/e19030105.

[59] Ermak DL, McCammon JA. Brownian dynamics with hydrodynamic interactions. J Chem Phys 1978;69:1352–60. https://doi.org/10.1063/1.436761.

[60] Tokuyama M, Oppenheim I. Dynamics of hard-sphere suspensions. Phys Rev E 1994;50:R16–9. https://doi.org/10.1103/PhysRevE.50.R16.

[61] Tokuyama M. Mean-field theory of glass transitions. Phys A Stat Mech Its Appl 2006;364:23–62. https://doi.org/https://doi.org/10.1016/j.physa.2005.08.041.

[62] Tokuyama M, Moriki T, Kimura Y. Self-diffusion of biomolecules in solution. Phys Rev E 2011;83:51402. https://doi.org/10.1103/PhysRevE.83.051402.

[63] Amsden B. An obstruction-scaling model for diffusion in homogeneous hydrogels. Macromolecules 1999;32:874–9. https://doi.org/10.1021/ma980922a.

[64] Belloni L, Drifford M TP. Counterion diffusion in polyelectrolyte solutions. Chem Phys 1984;83:147–54. https://doi.org/10.1016/0301-0104(84)85229-5.

[65] Xu Q, Boylan NJ, Suk JS, Wang Y-Y, Nance EA, Yang J-C, et al. Nanoparticle diffusion in, and microrheology of, the bovine vitreous ex vivo. J Control Release 2013;167:76–84. https://doi.org/10.1016/j.jconrel.2013.01.018.

[66] Lai SK, Wang Y-Y, Hida K, Cone R, Hanes J. Nanoparticles reveal that human

cervicovaginal mucus is riddled with pores larger than viruses. Proc Natl Acad Sci U S A 2010;107:598–603. https://doi.org/10.1073/pnas.0911748107.

[67] Hansing J, Duke JR, Fryman EB, DeRouchey JE, Netz RR. Particle Diffusion in Polymeric Hydrogels with Mixed Attractive and Repulsive Interactions. Nano Lett 2018;18:5248–56. https://doi.org/10.1021/acs.nanolett.8b02218.

[68] Hansing J, Duke JR, Fryman EB, DeRouchey JE, Netz RR. Particle Diffusion in Polymeric Hydrogels with Mixed Attractive and Repulsive Interactions. Nano Lett 2018;18:5248–56. https://doi.org/10.1021/acs.nanolett.8b02218.

[69] Shin J, Cherstvy AG, Metzler R. Sensing Viruses by Mechanical Tension of DNA in Responsive Hydrogels. Phys Rev X 2014;4:21002.

[70] Siepmann J, Siepmann F. Modeling of diffusion controlled drug delivery. J Control RELEASE 2012;161:351–62. https://doi.org/10.1016/j.jconrel.2011.10.006.

[71] Kosmidis K, Argyrakis P, Macheras P. A reappraisal of drug release laws using Monte Carlo simulations: The prevalence of the Weibull function. Pharm Res 2003;20:988–95. https://doi.org/10.1023/A:1024497920145.

[72] Kosmidis K, Macheras P. On the dilemma of fractal or fractional kinetics in drug release studies: A comparison between Weibull and Mittag-Leffler functions. Int J Pharm 2018;543:269–73. https://doi.org/10.1016/j.ijpharm.2018.03.060.

[73] Villalobos R, Garcia E V, Quintanar D, Young PM. Drug Release from Inert Spherical Matrix Systems Using Monte Carlo Simulations. Curr Drug Deliv 2017;14:65–72. https://doi.org/10.2174/2213476X03666160525144455.

[74] Maroto-Centeno JA, Quesada-Pérez M. Coarse-grained simulations of diffusion controlled release of drugs from neutral nanogels: Effect of excluded volume interactions. J Chem Phys 2020;152:024107. https://doi.org/10.1063/1.5133900.

[75] Aguirre G, Villar-Alvarez E, Gonzalez A, Ramos J, Taboada P, Forcada J. Biocompatible Stimuli-Responsive Nanogels for Controlled Antitumor Drug Delivery. J Polym Sci PART

A-POLYMER Chem 2016;54:1694–705. https://doi.org/10.1002/pola.28025.

[76] Alvarez-Bautista A, Duarte CMM, Mendizabal E, Katime I. Controlled delivery of drugs through smart pH-sensitivenanohydrogels for anti-cancer therapies: synthesis, drug release and cellular studies. Des MONOMERS Polym 2016;19:319–29. https://doi.org/10.1080/15685551.2016.1152542.

[77] Cazares-Cortes E, Espinosa A, Guigner J-M, Michel A, Griffete N, Wilhelm C, et al. Doxorubicin Intracellular Remote Release from Biocompatible Oligo(ethylene glycol) Methyl Ether Methacrylate-Based Magnetic Nanogels Triggered by Magnetic Hyperthermia. ACS Appl Mater Interfaces 2017;9:25775–88. https://doi.org/10.1021/acsami.7b06553.

[78] Gelissen APH, Scotti A, Turnhoff SK, Janssen C, Radulescu A, Pich A, et al. An anionic shell shields a cationic core allowing for uptake and release of polyelectrolytes within core-shell responsive microgels. Soft Matter 2018;14:4287–99. https://doi.org/10.1039/c8sm00397a.